Eur Biophys J (2005) 34: 890–898
DOI 10.1007/s00249-005-0459-y

ARTICLE

Sune Nørhøj Jespersen · Michael Pedersen
Hans Stødkilde-Jørgensen

The influence of a cellular size distribution on NMR diffusion measurements

Received: 7 June 2004 / Revised: 5 January 2005 / Accepted: 14 January 2005 / Published online: 11 May 2005

Abstract In the magnetic resonance community, the usefulness of diffusion-weighted imaging is undisputed. However, the correct interpretation of multicomponent diffusion is not widely agreed upon, and progress in this direction is impeded by several confounding experimental results. It is thus of great importance to resolve possible interfering factors. The objective of the present study is to examine the influence of a cellular size distribution. Using the Kärger equations, numerical calculations show that even substantial cellular size variations induce only small changes in the estimated compartmental diffusion constants and volume fractions.

Keywords Diffusion · Nuclear magnetic resonance · Cellular exchange time

Introduction

Although diffusion-weighted proton magnetic resonance imaging is of great clinical value, for instance, in diagnosing a stroke (Moseley et al. 1990), current understanding of the underlying biophysics is limited. Several candidate explanations point to the possible role of compartmental diffusion (Szafer and coworkers 1995a, 1995b; Latour et al. 1994; Schwarez et al. 2004): biexponential or multiexponential diffusion is ubiquitously observed in biological tissues. Whereas there is general agreement that this is due to the existence of two or more proton populations with different diffusional properties, the identity of the corresponding proton pools remains unclear (Schwarez et al. 2004; Clark and Bihan 2000; Lee and Springer 2003). In order to make further progress it is important to investigate the theoretical framework in which experimental data are analyzed. This is where numerical simulations (Meier 2003; Szafer 1995b; Latour et al 1994; Stanisz et al. 1997; Regan and Kuchel 2000, 2003) play a central role, because various physical mechanisms can be addressed individually and under ideal conditions. One such mechanism is the influence of heterogeneity on magnetic resonance diffusion measurements (Johnson 1998). Postprocessing of experimental data is typically done under the assumption of a single well-defined value of physical parameters such as the cellular diffusion constant, the radius and permeability, but in biological material one is likely to find a distribution of these parameters. This may be of less importance when the two-site exchange paradigm is just a convenient approximation, but if information on the true diffusion parameters is sought, the effects of polydispersity are unknown. The purpose of this study is to introduce a framework in which such a system can be analyzed, and to use it to investigate the influence of cell size polydispersity on pulsed field gradient diffusion measurements. We adapted the Kärger equations to model diffusion of water in a multicompartmental system, with one extra cellular compartment and a number of intracellular compartments each representing cells of the same type but of different sizes. In this model the cell sizes affect the signal as a result of their influence on the cellular exchange time. Therefore we begin in the ''Theory'' section with a discussion of the cellular exchange time and its dependence on physical parameters such as cell wall permeability, cell volume, and the intracellular diffusion constant. We arrive at a universal one-variable scaling function before specializing to spherical cells. For this particular cell shape we present an exact expression relating the cellular exchange time to the dependent variables. In the section ''Pulsed field gradient spin echo NMR diffusion'' we detail the model and its numerical implementation. Finally, we present our results and give our conclusions.

S. N. Jespersen (✉) · M. Pedersen · H. Stødkilde-Jørgensen
MR-Research Center, Aarhus University Hospital,
Brendstrupgaardsvej, 8200 Aarhus N, Denmark
E-mail: sune@mr.au.dk

Theory

The cellular exchange time τ is the average time spent by a diffusing particle inside a cell, and is in general dependent on the cell wall permeability κ, the intracellular diffusion constant D, the cell volume V, and the cell geometry. Formally,

$$\tau = T_{\text{shape}}(D,\ \kappa,\ V), \tag{1}$$

where T_{shape} is an unknown function, the form of which depends on the shape of the cell. Consider now the effect of space and time transformations on τ. Thus by letting $V' = V\lambda^3$ and $t' = \mu t$ we scale all distances by λ and time by μ, and therefore $\tau' = \mu\tau$. The remaining arguments of T_{shape} change according to

$$D' = \frac{D\lambda^2}{\mu} \quad \text{and} \quad \kappa' = \frac{\kappa\lambda}{\mu}. \tag{2}$$

This is valid for all choices of λ and μ, so we set $\lambda = V^{-1/3}$ and $\mu = \kappa\lambda$. After an appropriate redefinition of T_{shape}, we end up with the scaling form:

$$\tau = \frac{V^{1/3}}{\kappa} T'_{\text{shape}}\left(\frac{V^{1/3}\kappa}{D}\right). \tag{3}$$

Starting from a function of three independent variables, we have reduced the exchange time to a function of only one dimensionless scaling variable $x = V^{1/3}\kappa/D$. Moreover, physical arguments restrict the general asymptotic form of this function:

$$T'_{\text{shape}}(x) \sim \begin{cases} x & x \to \infty \\ \text{constant} & x \to 0. \end{cases} \tag{4}$$

Independent of the specific cell shape and in the limit of large cell wall permeability, the exchange time is determined by the time it takes for a molecule to travel a distance comparable to the cell size. Therefore, $\tau \propto V^{2/3}/D$, and this corresponds to the large x limit in Eq. 4. For a vanishing cell wall permeability, on the other hand, the exchange time is limited by the permeability and is given by the well-known formula $\tau = V/(A\kappa)$. The area A can be converted to a quantity of dimension $V^{2/3}$ (multiplied by a shape-dependent constant), and this yields the $x \to 0$ limit in Eq. 4.

As an example, consider a spherical cell with radius R. In that case Eq. 3 becomes

$$\tau = \frac{R}{\kappa} T'_{\text{sphere}}\left(\frac{R\kappa}{D}\right). \tag{5}$$

In fact, τ can be calculated exactly in this situation. Using results from Crank (1995), we obtain

$$\tau = 6\left(\frac{R^3\kappa^2}{D^3}\right)\sum_{n=1}^{\infty} \frac{1}{\beta_n^4\left[\beta_n^2 + x(x-1)\right]}, \tag{6}$$

where $\beta_n(x)$ is given as the solution to

$$\beta_n \cot(\beta_n) + x = 1 \tag{7}$$

and

$$x = \frac{R\kappa}{D}. \tag{8}$$

By reorganizing the analytical result, we can readily verify the scaling form in Eq. 5. This expression is exact, and numerical values for the exchange time can thus be obtained to arbitrary precision. The result has been compared with that from extensive Monte Carlo simulations of diffusion in spherical cells, and has been found to agree very well with the data (not shown). In addition, one may readily verify that the asymptotic form in Eq. 4 is fulfilled. Another expression for τ was given by Ash et al. (1978) and Kärger et al. (1978), which in our notation corresponds to

$$T'_{\text{sphere}}(x) = \frac{x}{15} + \frac{1}{3}. \tag{9}$$

Figure 1 illustrates the behavior of the scaling function calculated numerically from Eqs. 5, 6, 7, and 8, Eq. 9, and a one-term approximation from Sehy et al. (2002). The agreement of the linear expression from Eq. 9 with Eq. 6 is excellent, whereas the one-term approximation is acceptable only for small x.

We emphasize that the scaling form in Eq. 3 applies to all cell shapes, and this result may simplify studies of the cellular exchange time for more complicated cell shapes, such as the red blood cell studied by Regan and Kuchel (2000).

Pulsed field gradient spin echo NMR diffusion

It is evident from Eq. 3 that any variation in D, κ or R will bring about a similar variation in cellular water exchange times. In this section we consider the influence

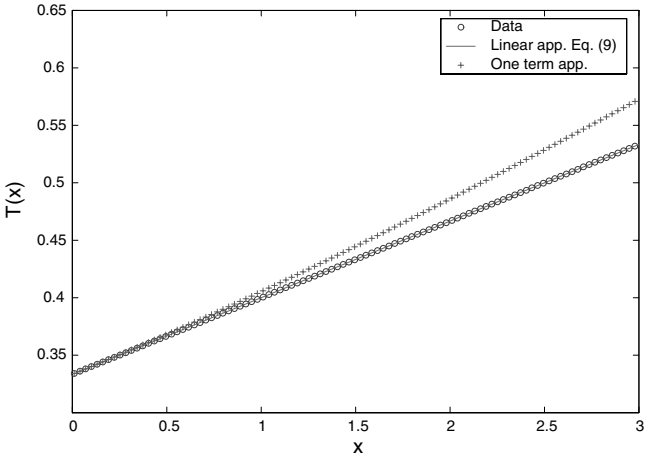

Fig. 1 Numerical calculation of the scaling function $T'_{\text{sphere}}(x)$ (Eqs. 5, 6, 7, 8), compared with the linear approximation (Eq. 9) and a one-term approximation (Sehy et al. 2002)

of such a variation on NMR diffusion measurements using the Kärger equations (Kärger et al. 1988). This model is based on the Chapmann–Kolmogorov equations and it describes the signal $S = S_1 + S_2 + \ldots + S_N$ arising from N proton exchanging compartments in a pulsed field gradient spin echo (Tanner and Stejskal 1968; Tanner 1978; Stejskal and Tanner 1965) experiment as the solution to

$$\dot{S}_i = -D_i q^2 S_i - \frac{S_i}{\tau_i} + \sum_{n \neq i} \frac{S_n p_{ni}}{\tau_n}, \quad i = 1, \ldots, N. \tag{10}$$

In this equation, D_i is the diffusion constant and τ_i the exchange time of the ith compartment, and $q = \gamma G \delta$ for a diffusion gradient of strength G and duration δ (see Fig. 2 for an illustration); γ is the gyromagnetic ratio. The p_{ij} designate the probability for a particle to enter compartment j upon leaving compartment i. In order for these equations to have an equilibrium solution, a set of constraints must be obeyed:

$$\frac{p_i}{\tau_i} = \sum_{n \neq i} \frac{p_n p_{ni}}{\tau_n}, \quad i = 1, \ldots, N, \tag{11}$$

where $p_n = S_n(0)$ denotes the relative particle number of compartment n.

It is important to note that the Kärger model is based on a number of assumptions. Notably, each compartment is essentially considered an infinite reservoir in which free diffusion takes place. Furthermore magnetization decay is not accounted for. Although this is an important effect in practice, especially when the different compartments have different decay rates, this is not the main focus of the present study, but it has been considered elsewhere (Vestergaard-Poulsen et al. 2004; Momot and Kuchel 2003). Hence, we will neglect longitudinal and transversal relaxation in the following. However, the results will be compared with those from a single simulation of a two-compartment system having different intracellular and extracellular T_2 values.

Two compartments are typically considered in magnetic resonance studies, corresponding, for example, to the intracellular and extracellular space. In this case the Kärger equations can be solved exactly (Kärger et al. 1988):

$$S(t) = S_1(t) + S_2(t) = p_1 {}^* \mathrm{e}^{-q^2 \mathrm{ADC}_1 t} + p_2 {}^* \mathrm{e}^{-q^2 \mathrm{ADC}_2 t}, \tag{12}$$

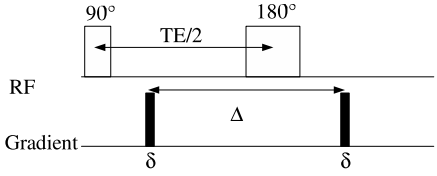

Fig. 2 Pulse sequence diagram for a pulsed field gradient spin echo experiment. TE is the echo time and △ the time between the leading edges of the gradients

where

$$\mathrm{ADC}_{1(2)} = \tfrac{1}{2}\left(D_1 + D_2 + \tfrac{1}{q^2}\left(\tfrac{1}{\tau_1} + \tfrac{1}{\tau_2}\right) \mp \left\{\left[D_2 - D_1 + \tfrac{1}{q^2}\left(\tfrac{1}{\tau_1} + \tfrac{1}{\tau_2}\right)\right]^2 + \tfrac{4}{q^4 \tau_1 \tau_2}\right\}^{1/2}\right) \tag{13}$$

and

$$p_2^* = \tfrac{1}{\mathrm{ADC}_2 - \mathrm{ADC}_1}(p_1 D_1 + p_2 D_2 - \mathrm{ADC}_1), \quad p_1^* = 1 - p_2^*. \tag{14}$$

ADC is the apparent diffusion constant, and it depends on q (and thus on the gradient strength), as does p^*, the corresponding volume fraction. Equations 12, 13, and 14 are frequently used when analyzing diffusion data, and estimation of parameters of interest is achieved by least-squares fitting.

We consider here a multicomponent system, where each cell is represented by its own compartment. As long as all cells are identical, this approach yields results identical to the two-compartment model, but allowing cells to have different properties entails new results. Here we focus on spherical cells with a distribution of radii, and as a consequence of Eqs. 5 and 9, the cells will differ in the associated exchange times.

The Kärger equations in Eq. 10 are essentially rate equations of the form $\dot{\mathbf{S}} = A\mathbf{S}$ with the solution $\mathbf{S}(t) = \exp(At)\mathbf{S}(0)$. Here $\mathbf{S} = (S_1, S_2, \ldots, S_N)$ and $\mathbf{A}$ is a time-independent matrix which can be read off directly from Eq. 10. Thus, the signal $S(t)$ is given by

$$S = \mathbf{e} \cdot \mathbf{S} = \mathbf{e} \cdot \exp(\mathbf{A}t)\mathbf{S}(0), \tag{15}$$

where $\mathbf{e} = (1, 1, \ldots, 1)$. In the case of one extracellular compartment in exchange with $N-1$ cellular compartments, $\mathbf{A}$ reads

$$\mathbf{A} = \begin{bmatrix} -D_\mathrm{e} q^2 - 1/\tau_\mathrm{e} & 1/\tau_1 & 1/\tau_2 \cdots & 0 \\ p_{\mathrm{e}1}/\tau_\mathrm{e} & -D_1 q^2 - 1/\tau_1 & 0 \cdots & 0 \\ p_{\mathrm{e}2}/\tau_\mathrm{e} & 0 & -D_2 q^2 - 1/\tau_2 \cdots & 0 \\ \vdots & \vdots & \vdots & \\ p_{\mathrm{e}N-1}/\tau_\mathrm{e} & 0 & \cdots & -D_{N-1} q^2 - 1/\tau_{N-1} \end{bmatrix}. \tag{16}$$

We have labeled the compartments such that subscript e refers to the extracellular space and $i = 1,\ldots,N-1$

to the cells. We assume no direct water exchange between the cells, and a schematic illustration of such a system, which is known as a mammillary system, is shown in Fig. 3.

The signal $S(t)$ is calculated as follows. We begin by generating the radius of each cell by sampling a normal distribution with mean radius $R = 6$ μm and standard deviation σ. Negative radii are discarded, and the radius is resampled from the distribution until a positive radius is returned. The matrix $\mathbf{A}$ is then constructed according to Eq. 16, and the solution is calculated from the exponentiation of $\mathbf{A}t$ as described by Eq. 15. We begin with constant gradient experiments, where the signal is calculated as a function of t with fixed q. Constant time experiments, where the strength of the diffusion gradient is varied, do not display a simple biexponential decay as a function of q^2. However, because of practical issues and certain other advantages (Cabrita et al. 2002), constant time experiments are more common than constant gradient experiments, and therefore we will treat them in a separate section. Simulations were performed with $D_e = 1.3$ μm^2 s^{-1}, $D_i = 0.05$ μm^2 s^{-1}, $\tau_e = 125$ ms, and the intracellular exchange time τ_i is calculated individually for each cell from its radius using Eqs. 5, 6, 7, and 8. The cellular water permeability is 4.42×10^{-2} μm ms^{-1}. The conditional transition probability $p_{e\,i}$ for a particle to enter a specific cell i from the extracellular space is calculated as the relative cellular surface area.

The constraints in Eq. 11 have the solutions

$$p_e = \frac{\tau_e}{\sum_i p_{ei}\tau_i + \tau_e} \tag{17}$$

and

$$p_e = \frac{\tau_e}{\sum_i p_{ei}\tau_i + \tau_e}, \quad i = 1, \ldots, N-1, \tag{18}$$

which determine the initial value $(S_e(0), \ldots, S_{N-1}(0))$. Using these constraints and the expression for the exchange time in Eqs. 6, 7, and 8, we found the cellular volume fraction to be $p_e = 0.8$ in the $\sigma = 0$ case (i.e., when all cells have the same radius of 6 μm). The values of the simulation parameters as given here were selected in a biologically realistic range, but were not chosen to model a specific tissue.

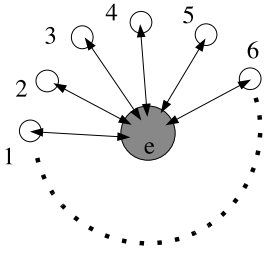

Fig. 3 Schematic illustration of a mammillary exchange system, with a population of $N-1$ cells and the extracellular space (denoted e). Water molecules do not travel directly from one cell to another, but have to pass through the extracellular space

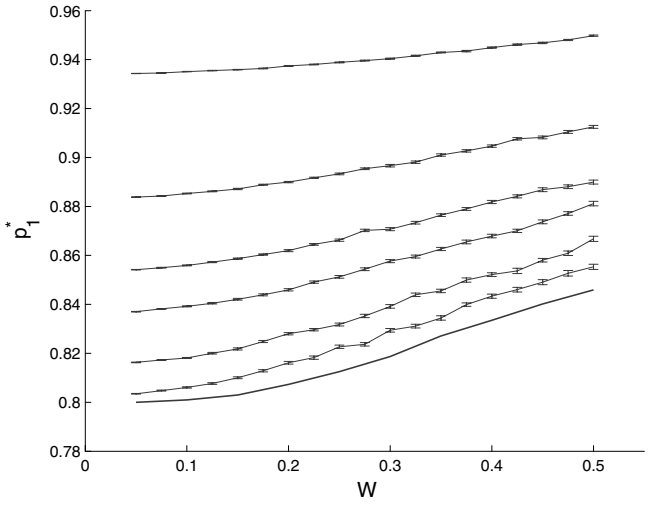

Fig. 4 Variation of p_i^* versus W, and $q = 0.1$, 0.15, 0.2, 0.25, 0.4, and 1 μm^{-1} from *top* to *bottom*. The *solid line* is the true intracellular volume fraction calculated from the cellular size distribution

Results

Constant gradient experiments

We define the parameter $W \equiv \sigma/R$ (sometimes known as the coefficient of variation) as the width of the radius distribution relative to the mean cellular radius. To analyze the influence of cell size variations on the interpretation of diffusion NMR measurements, we consider the implications of fitting the biexponential model in Eq. 12 to the numerical data. For each set of the simulation parameters we generate the signal $S(t)$ for

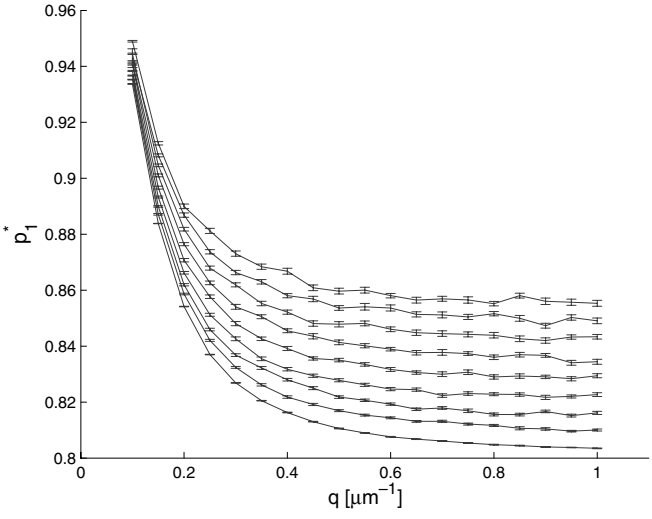

Fig. 5 Variation of p_i^* versus q for $W = 0.05$, 0.15, 0.2, 0.25, 0.3, 0.35, 0.4, 0.45, and 0.5 from *bottom up*. The $W = 0$ case would be only barely distinguishable from the $W = 0.05$ case (data not shown)

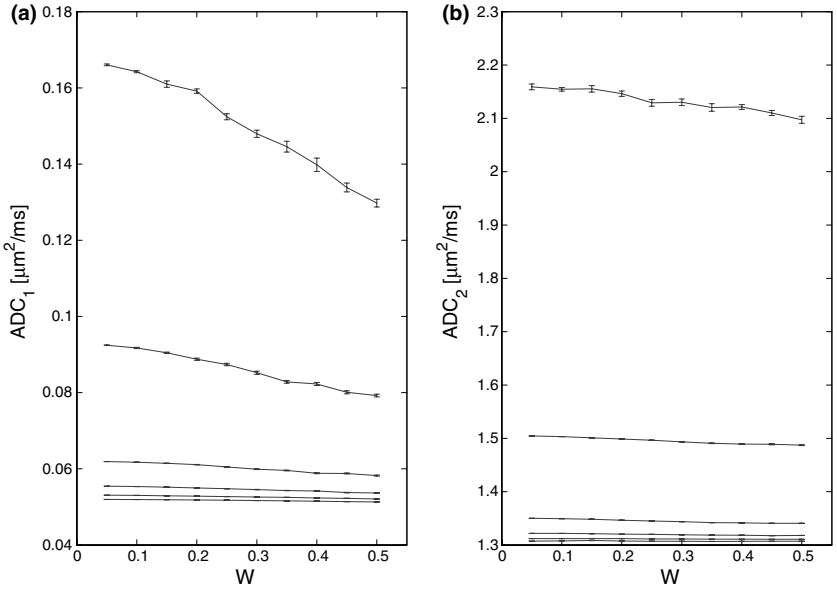

Fig. 6 Variation of ADC_1 (**a**) and ADC_2 (**b**) versus W, and $q = 0.1$, 0.15, 0.2, 0.25, 0.4, and 1 μm^{-1} from *top down*. *ADC* apparent diffusion constant

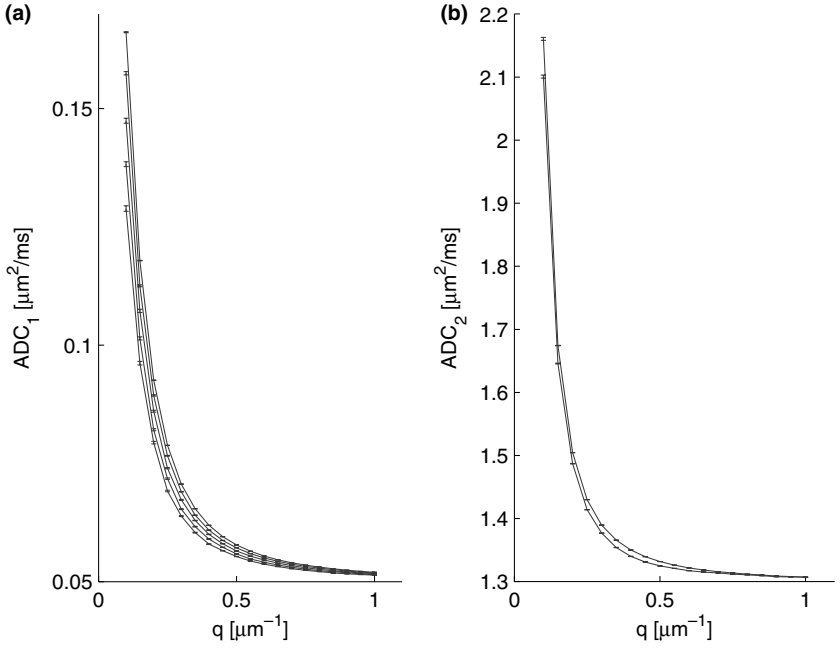

Fig. 7 Variation of ADC_1 (**a**) versus q for $W = 0.05$, 0.2, 0.3, 0.4, and 0.5 from *top down*, and ADC_2 (**b**) versus q for $W = 0.05$ (*upper curve*) and 0.5

$t = 0$, 2,..., 200 ms and fit Eq. 12 to the data with p_2^*, ADC_1, and ADC_2 as free parameters, and p_2^* determined by the normalization constraint $p_1^* + p_2^* = 1$. The indices were chosen such that subscript 1 refers to the cellular and subscript 2 to the extracellular compartment. We repeated the procedure 40 times and averaged the resulting fit parameters.

In Fig. 4 we plot p_1^* versus W for $q = 0.1$, 0.15, 0.2, 0.25, 0.4, and 1 μm^{-1}. We observe a systematic dependence of the relative compartment fractions on W, leading to an apparently increasing cellular compartment and a decreasing extracellular volume. The change is most pronounced for high q values, where p_1^* is higher by 6% and p_2^* is lower by as much as 25%, representing a rather significant impact on the extracellular fraction. Low q values reflect large spatial distances, and generally in this limit $p_1^* \to 1$ and $p_2^* \to 0$ according to Eq. 13: in other words, the diffusing particles effectively see only one compartment having a volume fraction of 1 in this limit. Therefore it is not surprising that the high-q regime is more sensitive to variations in compartmental volumes than the low-q regime.

However, the deviation of the compartment volumes from the ideal $W = 0$ case is only partially due to the imposed two-compartment description: there is a real dependence of the volumes on W which is also reflected in these numbers. As stated earlier, we chose the parameters such that, in the absence of any cell size variations, the cellular fraction is exactly 0.8. However, in this model a nontrivial cell size distribution will

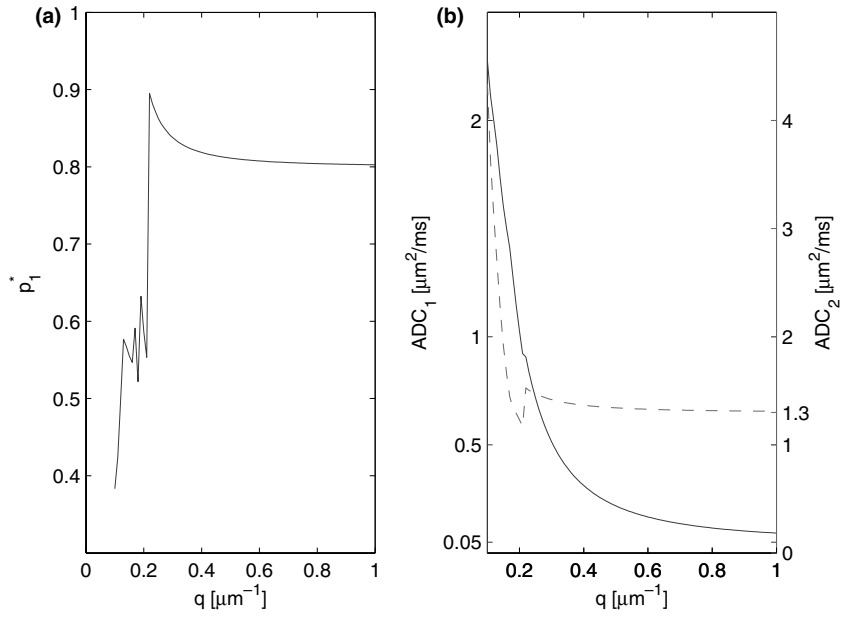

Fig. 8 Estimated diffusion parameters for a two-component system with different T_2 relaxation rates. The estimated intracellular volume fraction (**a**) behaves somewhat erratically around $q = 0.2$ μm^{-1}. (**b**) The estimated diffusion constants ADC$_1$ (*solid line*) and ADC$_2$ (*dashed line*) are plotted as a function of q

change this value, and in Fig. 4 we have included the results from a numerical calculation of the actual intracellular volume fraction (solid line). As can be seen, the two lowest curves follow each other closely, but there is a systematic overestimation (underestimation) of the cellular (extracellular) volume fraction; however, this effect is relatively small, and nowhere does it exceed 2% for the cellular volume fraction. Therefore, in spite of an underlying multicompartment system, a two-compartment description appears to be sufficiently precise for determining the cellular volume fraction.

In Fig. 5 we reorder the data from Fig. 4 and plot them as a function of q. Again a significant systematic dependence on W is observed. On the other hand, if we compare the qualitative behavior of p_1^* versus q with the one expected, viz. Eq. 14, from the two-compartment model, it is hardly distinguishable from the $W = 0.05$ curve (data not shown).

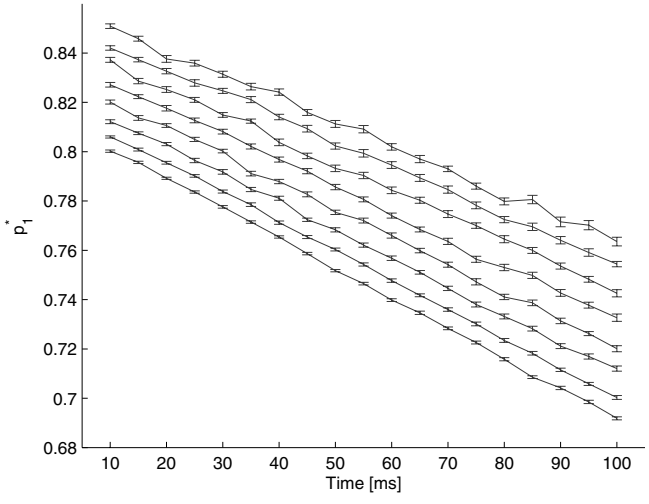

Fig. 9 Estimated intracellular volume fraction as a function of diffusion time and $W = 0.5$, 0.45, 0.4, 0.35, 0.3, 0.25, 0.2, 0.15 and 0.05 from *top down*

We plot the two remaining parameters, ADC$_1$ and ADC$_2$, versus W in Fig. 6. A decreasing trend is observed, and we note that by far the largest effect is seen for ADC$_1$ (intracellular diffusion) and for the low q values. For the largest q values, for which the apparent diffusion constants approach the true diffusion constants, the effect of a nonvanishing W on ADC$_1$ and ADC$_2$ is minuscule.

We replot the data as a function of q in Fig. 7. This figure confirms that the ADCs are most sensitive to cell size variations for low q values. This is reasonable since for high q values, the ADC reflects more accurately the true diffusion constants (Eq. 13), thus reducing the influence of the exchange times in this limit. In summary, both ADCs are generally overestimated compared with the true diffusion constant, but increasing polydispersity will decrease this overestimation, and more so the lower the q value.

Disagreement between various groups concerning the value of ADCs can therefore hardly be attributed to cell size variations. More significant is the influence of too low q values. This can itself be investigated by repeating the experiment for several q values: only when there is no substantial q variation in the ADCs is it comparable to the physical diffusion constants. And in this case, cellular size heterogeneity should only affect the estimated diffusion constants minimally. In fact, it is interesting to note that polydispersity tends to decrease the overestimation of the ADCs stemming from insufficiently high q values (Fig. 8).

In Fig. 9, p_1^*, ADC$_1$ and ADC$_2$ are plotted as a function of q for a two-compartment system with an intracellular T_2 of 25 ms and an extracellular T_2 of 400 ms. All other parameters are the same as before and $W = 0$. As is evident from this figure, the effect of

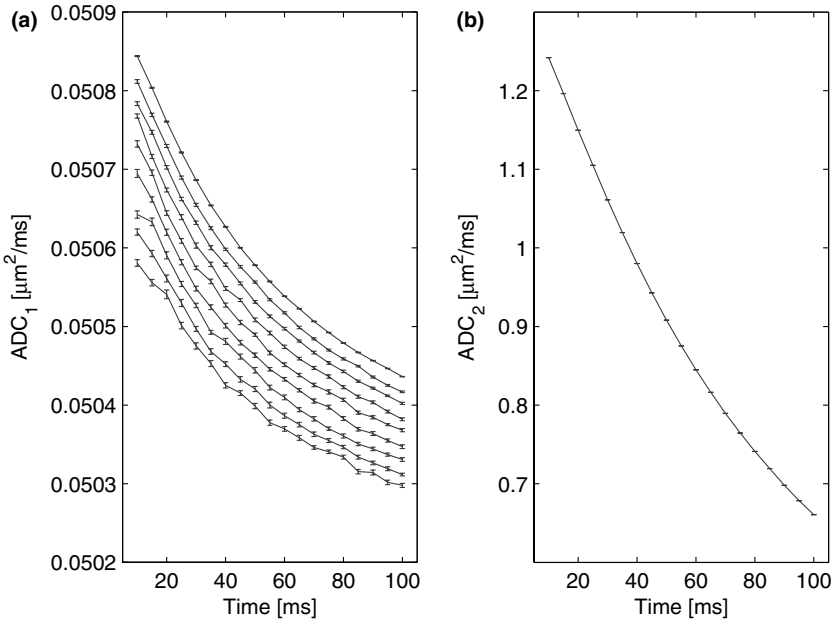

Fig. 10 ADCs as a function of diffusion time. (**a**) ADC_1 for $W = 0.05$, 0.15, 0.2, 0.25, 0.3, 0.35, 0.4, 0.45, and 0.5, and (**b**) ADC_2 for $W = 0.05$ and 0.5 from the *top down*

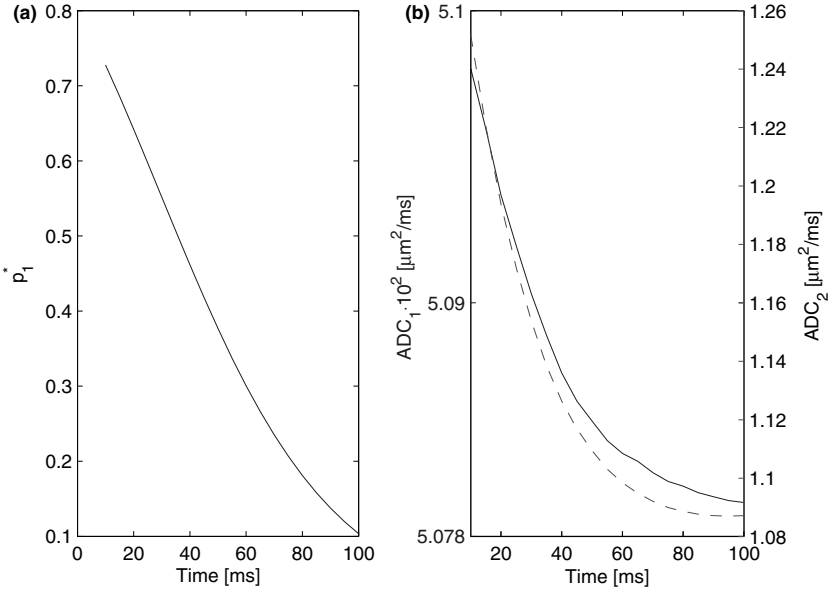

Fig. 11 Simulation data from the two-compartment system with different transversal relaxation rates. (**a**) The intracellular volume fraction and (**b**) the ADCs (ADC_1 *solid line* and ADC_2 *dashed line*)

differing transversal relaxation times can be much more significant than the effect of cellular polydispersity. However, as q increases, the diffusion parameters approach the true values.

Constant time experiments

In this section the experimentally more widespread situation of constant time experiments is studied. The signal from the Kärger model is not biexponential in this case, but multiexponential, but in practice a biexponential function fits very well. In the following, the signal is obtained as a function of q from $q = 0\ \mu m^{-1}$ to $q = 1\ \mu m^{-1}$, and for a range of diffusion times $t = 10$–100 ms and polydispersities $W = 0.05$–0.5. The same procedure as in the previous section was employed: the fit parameters (p_1^*, ADC_1, ADC_2) from 40 realizations were averaged, and the error bars on the curves are standard errors. It was found that fitting the logarithm of the data to the logarithm of Eq. 12 yielded somewhat better fits, and this procedure was therefore adopted.

The apparent intracellular volume fraction increased in samples of increasing polydispersity (Fig. 9), as for the constant gradient experiments. For experiments with small diffusion times, this reflects the behavior of the

true intracellular volume fraction, included in Fig. 4. As the diffusion time increases however, the apparent intracellular volume fraction is increasingly underestimated. This effect is seen even on monodisperse samples, and in fact the relative error of p_1^* for a given diffusion time becomes smaller with increasing polydispersity.

Figure 10 shows the apparent diffusion constants as a function of t. The intracellular diffusion constant ADC_1 ($D_1 = 0.05$ μm^2 ms^{-1}) is slightly overestimated for all values of t and W. The variability in ADC_1 as a function of W is roughly similar to the variability as a function of t. For the extracellular diffusion constant, however, there are barely any effects of polydispersity. The decrease in ADC_2 as a function of diffusion time is quite significant, and results in a large underestimation of the true extracellular diffusion constant ($D_2 = 1.3$ μm^2 ms^{-1}).

For comparison, the diffusion parameters from a two-compartment system with differing T_2 relaxation times (intracelullar $T_2 = 25$ ms and extracellular $T_2 = 400$ ms) are shown in Fig. 11. The estimate of the intracellular volume fraction is significantly modified by the presence of two T_2 components, whereas the intracellular diffusion constant is quite unaffected (compare with Fig. 10).The extracellular diffusion constant also turns out to vary less than in the monoexponential T_2 case.

Conclusions

In this study, we investigated the effect of cellular size distributions on NMR diffusion measurements. We found that even a relatively broad distribution of cellular radii leads only to a relatively minor effect in the estimates of diffusion constants and volume fractions in the two-compartment model. For constant gradient experiments, the influence of diffusion gradients on the ADCs dominates. For constant gradient experiments, all parameters (p_1^*, ADC_1, ADC_2) were consistently overestimated; however, this effect was mainly due to low q values, and in fact for the ADCs, polydispersity counteracted this tendency. For constant time gradients on the other hand, a finite diffusion time resulted in an underestimation of the true intracellular volume fraction. The apparent intracellular diffusion constant was always larger than the true diffusion constant, whereas the extracellular diffusion constant was always smaller than the true extracellular diffusion constant. In both cases however, increasing polydispersity tended to decrease the values of the ADCs. The results were compared with those from simulations of a two-compartment model with the same parameters but having different T_2 relaxation rates. Failure to take this into account in the data analysis was seen to have a much greater impact on the estimation of some of the diffusion parameters.

We also considered the general theory of exchange time calculations for arbitrary cell shapes. We derived a one-variable scaling form which can be used to simplify future studies on cellular exchange time. This scaling form compared favorably to the results for spherical cells, for which we also derived an exact expression relating the exchange time to the cellular radius, the diffusion constant, and the cell wall permeability.

Further studies are needed in order to clarify the consequences of variations in cellular diffusion constants and permeabilities, as well as compartmental differences in, for example, transversal relaxation rates. It may be interesting in this respect to compare the predictions of the Kärger model with the outcome of first principles Monte Carlo simulations. In addition, it is important to acquire experimental data from biological samples which can be well characterized on a cellular level.

References

Ash R, Barrer R, Craven R (1978) Sorption kinetics and time-lag theory. J Chem Soc Faraday II 74:40–56

Cabrita E, Berger S, Brauer P, Karger J (2002) High-resolution dosy nmr with spins in different chemical surroundings: Influence of particle exchange. J Magn Reson157:124–131

Clark C, Bihan DL (2000) Water diffusion compartmentation and anisotropy at high b values in the human brain. Magn Reson Med 44(6):852–859

Crank J (1995) The mathematics of diffusion. Clarendon Press, Oxford

Johnson C (1998) Diffusion ordered nuclear magnetic resonance spectroscopy: principles and applications. Prog Nuclear Magn Reson Spectrosc 34:203–256

Kärger J, Pfeifer H, Heink W (1988) Principles and applications of selfdiffusion by nuclear magnetic resonance. Adv Magn Res 12:1–89

Latour L, Svoboda K, Mitra P, Sotak C (1994) Time-dependent diffusion of water in a biological model system. Proc Natl Acad Sci USA 91(4):1229–1233

Lee J, Springer C (2003) Effects of equilibrium exchange on diffusionweighted NMR signals: the diffusigraphic ''shutter-speed''. Magn Reson Med 49(3):450–458

Meier C, Dreher W, Leibfritz D (2003) Diffusion in compartmental systems. I. A comparison of an analytical model with simulations. Magn Reson Med 50(3):500–509

Momot K, Kuchel P (2003) Pulsed field gradient nuclear magnetic resonance as a tool for studying drug delivery systems. Concepts Magn Reson Part A 19A:51–64

Moseley M, Cohen Y, Mintorovitch J, Chileuitt L, Shimizu H, Kucharczyk J, Wendland M, Weinstein P (1990) Early detection of regional celebral ischemia in cats; comparison of diffusion- and t2-weighted mri and spectroscopy. Magn Reson Med 14:330–346

Regan D, Kuchel P (2000) Mean residence time of molecules diffusing in a cell bounded by a semi-permeable membrane: Monte Carlo simulations and an expression relating membrane transition probability to permeability. Eur Biophys J 29(3):221–227

Regan D, Kuchel P, (2003) Simulations of NMR-detected diffusion in suspensions of red cells: the effects of variation in membrane permeability and observation time. Eur Biophys J 32(8):671–675

Schwarcz A, Bogner P, Meric P, Correze J, Berente Z, Pal J, Gallyas F, Doczi T, Gillet B, Beloeil J (2004) The existence of biexponential signal decay in magnetic resonance diffusion-weighted imaging appears to be independent of compartmentalization. Magn Reson Med 51(2):278–285

Sehy J, Banks A, Ackerman J, Neil J (2002) Importance of intracellular water apparent diffusion to the measurement of membrane permeability. Biophys J 83(5):2856–2863

Stanisz G, Szafer A, Wright G, Henkelman R (1997) An analytical model of restricted diffusion in bovine optic nerve. Magn Reson Med 37(1):103–111

Stejskal E, Tanner J (1965) Spin diffusion measurements: spin echoes in the presence of a time-dependent field gradient. J Chem Phys 42:288–292

Szafer A, Zhong J, Anderson A, Gore J (1995a) Diffusion-weighted imaging in tissues: theoretical models. NMR Biomed 8(7–8):289–296

Szafer A, Zhong J, Gore J (1995b) Theoretical model for water diffusion in tissues. Magn Reson Med 33(5):697–712

Tanner J (1978) Transient diffusion in a system partitioned by permeable barriers—application to nmr measurements with a pulsed field gradient. J Chem Phys 69:1748–1754

Tanner J, Stejskal E (1968) Restricted self-diffusion of protons in colloidal systems by pulsed-gradient spin-echo method. J Chem Phys 49:1768–1777

Vestergaard-Poulsen P, Laursen T, Jakobsen R, Hansen B, Østergaard L (2004) Transverse relaxation is important when modelling water self diffusion in brain tissue. In: Proceedings of ISMRM Twelfth Scientific Meeting, Kyoto